Numerical study of pendulums: From the simple pendulum approximation to the damped physical pendulum with variable mass

R. Espíndola-Heredia[1,2], G. del Valle[1] and G. Hernández[1]

[1]Departamento de Ciencias Básicas, Área de Física Atómica y Molecular, Universidad Autónoma Metropolitana Azcapotzalco, Av. San Pablo 180, Azcapotzalco, México D. F.

[2]Unidad Académica y Profesional de Cuautitlán Izcalli, Universidad Autónoma del Estado de México, Colonia Atlanta 2ª Sección, Cuautitlán Izcalli, Estado de México.

E-mail: respindolah@uaemex.mx

(Received 13 March 2012, accepted 26 June 2012)

Abstract

Using the numerical method of Runge-Kutta for systems of nonlinear ordinary differential equations of second order with initial conditions, we studied different systems: the simple pendulum, mathematical pendulum (without approximation of small angles), the damped pendulum (with damping constant ν), the physical pendulum (with moment of inertia $I = ⅓ML^2$), the physical pendulum damped (with the same moment of inertia and damping constant ν), the physical pendulum with variable mass (considering only one case: linear dependence of mass with respect to time) and finally the damping physical pendulum with variable mass. In all systems were studied different initial conditions, show some solutions for the position, velocity and the phase plane, and discusses some cases of interest.

Keywords: Physical Pendulum, Simulations, Variable Mass, Non Linear Differential Equations.

Resumen

Usando el método numérico de Runge-Kutta para sistemas de ecuaciones diferenciales ordinarias no lineales de segundo orden con condiciones iniciales, estudiamos sistemas diferentes: El péndulo simple, péndulo matemático (sin ninguna aproximación de ángulos pequeños) el péndulo amortiguando (con constante de amortiguamiento ν), el péndulo físico (con momento de inercia $I = ⅓ML^2$), el péndulo de amortiguamiento físico (con el mismo momento de inercia y constante de amortiguamiento ν), el péndulo físico con masa variable (considerando solo un caso: Dependencia lineal de masa con respecto al tiempo) y finalmente el péndulo de amortiguamiento físico con masa variable (En todos los sistemas fueron estudiadas condiciones iniciales diferentes), muestra algunas soluciones para la posición, velocidad y el plano de fase, y se analizan algunos casos de interés.

Palabras clave: Péndulo Físico, Simulaciones de Masa Variable, Ecuaciones Diferenciales No Lineales.

PACS: 02.60.Jh, 02.60.Cb, 01.55.+b **ISSN 1870-9095**

I. INTRODUCTION

In regular courses of basic physics is taught the pendulum motion. A pendulum is an oscillating system which rotates about a fixed point. It consists of a point mass (*m*) suspended from a string of length (*l*) and negligible mass that can´t stretch. If the mass is moved to one side of its equilibrium position, the wire form an angle θ with respect to the vertical, when released, the mass *m* oscillates around of this position. The equations governing this motion are equations where the position, velocity and acceleration are time dependent. The motion equation is a nonlinear ordinary differential equation (NODE), which can be written as follows:

$$\frac{d^2\theta(t)}{dt^2}+\frac{g}{l}Sin(\theta(t))=0, \qquad (1)$$

Usually in textbooks of both differential Eqs. [1, 2] such as those discussed numerical methods [3] for solving differential equations, only present the same case: the simple pendulum (SP), which is to assume that the angle θ is small and where can used the small-angle approximation: $Sin[\theta] \cong \theta$. So we can say that the movement of the pendulum is simple harmonic and that in studying the dynamics of their movement will get the period and frequency dependent only on the length and value of gravity.

$$\frac{d^2\theta(t)}{dt^2}+\frac{g}{l}\theta(t)=0. \qquad (2)$$

The other case studied in courses and in textbooks [4] correspond to the mathematical pendulum (MP), unlike SP, does not consider small angles and solves the NODE (1), the period of the pendulum depends not only on the length and value of gravity, but involves elliptic integrals of first kind. The analytical solution of Eq. (1) represents an academic exercise in the regular courses of intermediate physics.

In the literature there are also a variety of texts related to pendulums [4, 5, 6, 7, 8, 9, 10], are theoretical [5], experimental [6] and numerical results [7], such as: forced pendulum [8], physical pendulums [9], pendulum with variable length [10], and some have studied the issue of pendulums of mass variable [8, 11, 12, 13, 14]. In this paper, our purpose is to present the numerical solution based on the Runge-Kutta method to solve the NODE (1) for damped physical pendulum with variable mass. We start with a fairly known as SP and we compounded the problem by passing the MP, then we treat the physical pendulum (PhP) and then enter the buffer and get the solution of damped physical pendulum, and finally set the numerical solution damped physical pendulum with variable mass.

II. THEORY

The Eq. (1) can be solved analytically, which involves solving elliptic integrals. An alternative is to solve it through a numerical method. There are different algorithms that are used as integrators for the solution of an NODE, including the method of Euler where is necessary mentioned the Leap-Frog method, Taylor Series and Runge-Kutta, among many others. This latter are a set of iterative methods (implicit and explicit) to approximate NODE solutions specifically to initial value problem:

$$\frac{d^2 y(t)}{dt^2} \pm \frac{d\, y(t)}{dt} \pm y(t) = 0 \qquad \forall\ a \le t \le b$$
$$y(0) = \phi; \quad \dot{y}(0) = \xi. \tag{3}$$

The Runge-Kutta method is not only a reality but is an important family of iterative methods used to approximate the solutions of NODE, which highlights the Runge-Kutta method of fourth order. That being the most used and known, is referred to as the "Runge-Kutta method". Defining the method for the problem of initial values given in Eq. (3), then:

$$y_{i+1} = y_i + \tfrac{1}{6.0}\left(k_1 + 2.0k_2 + 2.0k_3 + k_4\right)\Delta h. \tag{4}$$

Where

$$\begin{aligned} k_1 &= f(x_i, t_i), \\ k_2 &= f(x_i + \tfrac{1}{2}\Delta h, t_i + \tfrac{1}{2}k_1\Delta h), \\ k_3 &= f(x_i + \tfrac{1}{2}\Delta h, t_i + \tfrac{1}{2}k_2\Delta h), \\ k_4 &= f(x_i + \Delta h, t_i + \tfrac{1}{2}k_3). \end{aligned} \tag{5}$$

Thus, the next value ($y_i + 1$) is determined by this value (y_i) plus the product of the interval size *(Δh)* for an estimated slope. The slope is a weighted average of slopes: k_1 is the slope at the beginning of the interval, k_2 is the slope at the midpoint of the interval, using k_1 to determine the value of y at the point using Euler's method, k_3 is again the slope of the midpoint, but now using k_2 to determine the value of y, k_4 is the slope at the end of the interval, with the value of y determined by k_3. Averaging the four slopes, greater weight is assigned to the slopes in the middle: This form of the Runge-Kutta is a method of fourth order which means that the error per step is about $\vartheta(\Delta h^5)$ while total accumulated error has order $\vartheta(\Delta h^4)$.

III. SIMULATION

To carry out the simulation of the expression (1) was necessary to make a change of variable:

$$\begin{aligned} &u_1(t) = \theta(t), \\ &u_2(t) = \frac{d}{dt}u_1(t) = \frac{d}{dt}\theta(t) \therefore \\ &\frac{d}{dt}u_2(t) = \frac{d^2}{dt^2}\theta(t). \end{aligned} \tag{6}$$

Thus obtains the following set of coupled equations:

$$\begin{aligned} &\frac{d}{dt}u_1(t) = u_2(t), \\ &\frac{d}{dt}u_2(t) = -\omega^2 Sin(u_1(t)), \end{aligned} \tag{7}$$

where $\omega^2 = \sqrt{(g/l)}$ and initial conditions are determined by:

$$\begin{aligned} u_1(t) &= \theta(t) = \phi, \\ u_2(t) &= \dot{\theta}(t) = \xi. \end{aligned} \tag{8}$$

We have done simulations for various systems. I) Simple Pendulum, II) Mathematical Pendulum, III) Damped Pendulum, IV) Physical Pendulum, V) Physical Pendulum Damped, VI) Variable Mass Physical Pendulum and VII) Physical Pendulum with Damping and Variable Mass. In all cases we take the value of gravity as $g = 9.81$m/s^2, the length $l = 1.0m$,

IV. RESULTS

SP. We worked the case I) as a calibration form to verify that our results were consistent, and that the expressions were correctly programmed. Numerically solved by changing the Eq. (7) the expression $Sin(u_1(t))$ by $u_1(t)$. The integration interval was $0 \le t \le 2.00607$, we generated

N=500 steps in that range, the size of temporal displacement was Δh = 0.004012. Were evaluated $n = 150$ different initial conditions, which were randomly generated for a range between the $-15°$-$\leq \varphi \leq 15°$, and $\xi = 0.0$.

We compared the solution given by the our simulation with the analytical solution, we find the same graph to the solution for the variables: $\theta(t)$ and $v(t)$, also then the phase plane was plotted in both cases and the compared the two solution were find identical. It also we obtained the value of the period of the pendulum corresponding to the value: $T = 2\pi/\omega$.

<u>MP</u>. The case II) was worked similarly, we solved numerically the Eq. (7) with the expression $Sin(u_1(t))$. The integration interval was $0 \leq t \leq 4.5$, we generate N = 1000 steps in that range, the size of temporal displacement was $\Delta h = 0.0045$. We evaluated n = 80 different initial conditions, which were randomly generated for a range between $-180^o \leq \varphi \leq 180°$, and $\xi=0.0$. Were compared the solution obtained by the simulation with the analytical solution, which solved the equation for the total energy $E = K + U$, as the system is conserved. Then the energy is given by:

$$E = \tfrac{1}{2} mv^2 + mgl\left[1.0 - Cos(\theta(t))\right]. \tag{9}$$

The solution was plotting, in the Fig. 1 shows the speeds as function of the angle $v(\theta)$, from Eq. (9), see Fig. 1, we found that the chaotic region is given to values higher mechanical energy $E = 19.62J$, and these were well reproduced by the simulation. In Fig. 1, the blue dots are the simulation results, while the curves with different colors corresponding to different values of the energy given by Eq. (9)

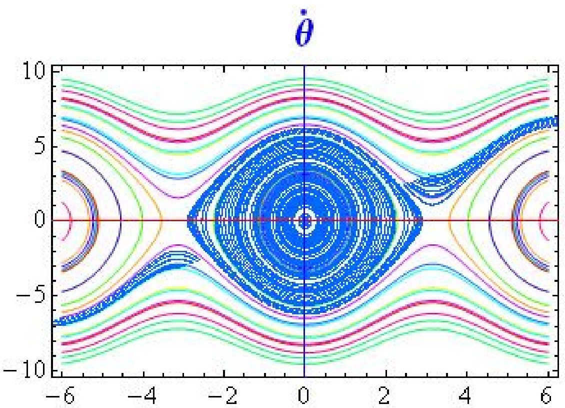

FIGURE 1. Phase diagram of the system I. Shows the comparisons between simulation and the theoretical expression.

<u>DP</u>. For the case III) enter into the Eq. (7) the damping factor given by $-bv$. The integration interval was $0 \leq t \leq 3.5$, were generated $N = 500$ steps in that range, the size of temporal displacement was $\Delta h = 0.007$. Were evaluated $n = 100$ different initial conditions, which were randomly generated for a range between $-25^o \leq \varphi \leq 25^o$, and $\xi = 0.0$. Fig. 2 shows the case where the damping constant b is given by $b = 2.0\sqrt{(g/l)}$, which describes the case of critical damping.

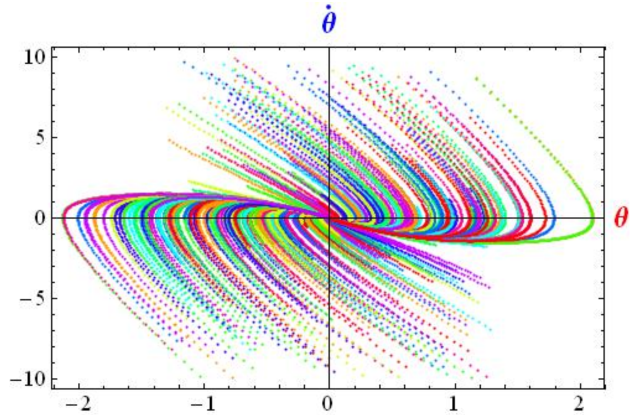

FIGURE 2. Phase diagram of system II with critical damping. $b= 2.0\sqrt{(g/l)}$.

The same way as for the case I, the phase plane was generated for this system with initial conditions above, not show the presence of the chaotic. Then we generate initial conditions for a wider range:$-180^o \leq \varphi \leq 180°$. Fig. 3 shows the relationship between the angle and time, there are curves representing a chaotic state.

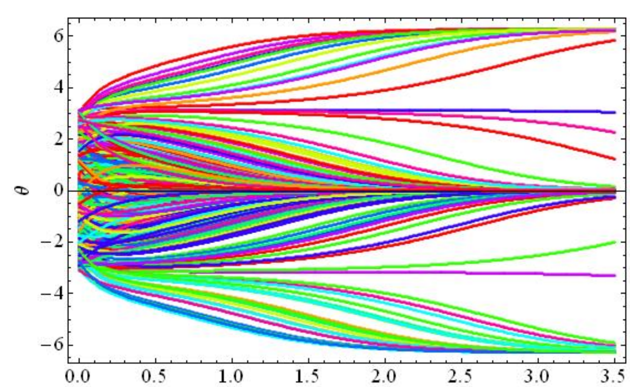

FIGURE 3. $\theta(t)$, for the case of critical damping initial conditions in a wider range.

The phase plane is presented in Fig. 4, also for 100 different initial conditions, it is possible to observe the chaotic regions and the existence of a stable region for the movement of the pendulum that describes a harmonic motion.

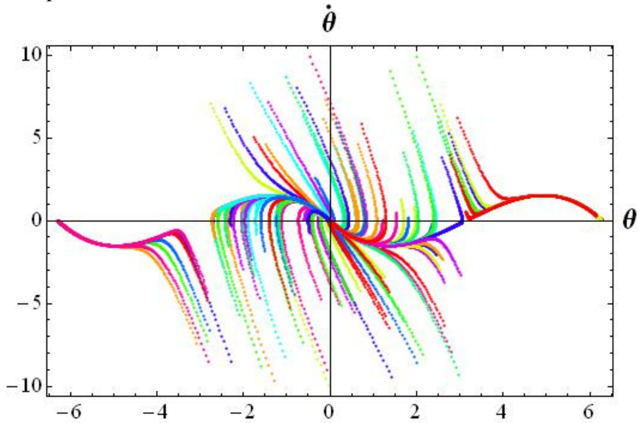

FIGURE 4. Phase diagram of the case shown in Fig. 3.

PhP. For the case IV) the Eq. (7) is unchanged with respect to the previous cases the equations used are as follows

$$I\frac{d^2\Theta(t)}{dt^2} - Mgd\,Sin\left[\Theta(t)\right] = 0. \qquad (10)$$

So that in Eq. (7) the value of the angular velocity ω^2 is replaced by *Mgd/I*, where *M* is the mass of physical pendulum, *d* is the distance from the center of mass to the axis of rotation, *I* is the moment of inertia a straight cylinder $I = ML^2/3$, *L* is the length of the cylinder. The integration interval for this case was $0 \le t \le 3.5$, we generate $N = 350$ steps in that range, the size of temporal displacement was $\Delta h = 0.01$ and $n = 500$ different initial conditions were evaluated, which were randomly generated for a range between $-35^o \le \varphi \le 35^o$ and $-1.5Mgd/I \le \varphi \le 1.5Mgd/I$. The value of the length of the cylinder was taken as $L=2$, so that the distance *d* is equal to unity. Fig. 5 shows the phase plane generated for this system. Which preserves the structure of the case II) as it should be.

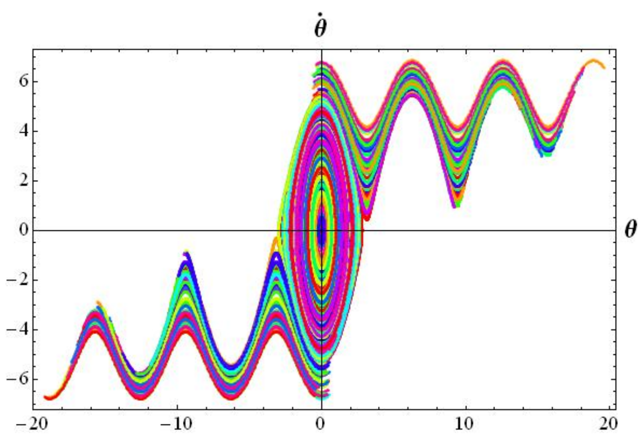

FIGURE 5. Diagram of the physical pendulum phase.

PhPD. For the case V) in Eq. (7) again introduce the damping factor given by *-bv*, the damping constant in this case has a value of $b = 0.75kg/s$, then introducing a weak buffer case. We solve the system with the integration interval $0 \le t \le 15$, we generated $N = 1000$ steps in that range, the size of temporal displacement was $\Delta h = 0.015$. We evaluated n =100 initial conditions randomly that were generated for a range: $-95^o \le \varphi \le 95^o$, and for speed: $-Mgd/I \le \xi \le Mgd/I$.

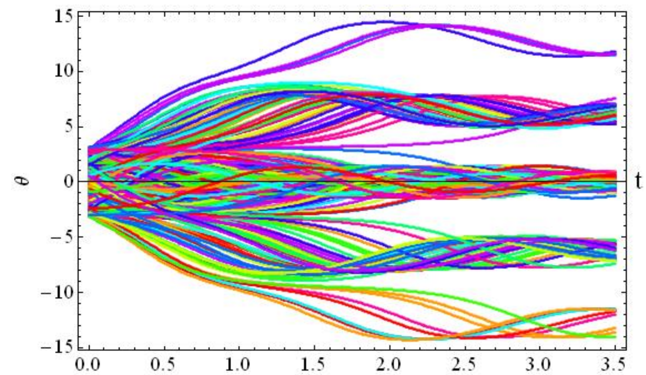

FIGURE 6. Angle versus time for the Physical Pendulum with Damping.

The Fig. 6 shows the graph of the angle versus time. There are 5 different equilibrium states where different paths converge. It also shows the damping of the system, because the oscillation is decaying. Fig. 7 shows the phase space where there are these 5 regions of stability are presented as system attractors and chaotic regions as well.

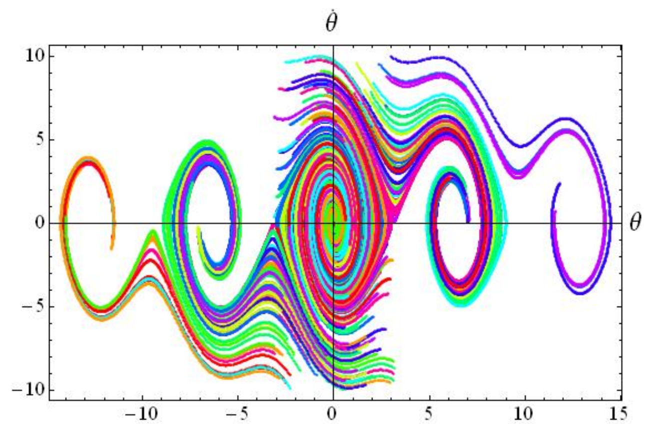

FIGURE 7. Phase diagram of the damped physical pendulum.

PhPMV. For the case VI) was necessary to introduce time dependence in the properties: mass, inertia moment and distance from the axis of rotation to mass center, which in previous cases have been constant. We follow the treatment done by G. del Valle and coworkers [14] and, assuming that the mass change is a linear dependence given as follows:

$$M_g(t)=\begin{cases} M_o\left(1.0-\left(\sqrt{\frac{g}{2.0\,L}}\right)t\right) & si\ \ t\le\sqrt{\frac{2.0\,L}{g}} \\ M_o\left(1.0-\left(\sqrt{\frac{g}{2.0\,L}}\right)\sqrt{\frac{2.0\,L}{g}}\right) si & t>\sqrt{\frac{2.0\,L}{g}} \end{cases}. \quad (11)$$

Where we assume that *Mg* is the mass of granular medium which is filled with the cylinder, the initial time t = 0, *Mg= Mo* it is the mass of granular material at the beginning, at time *t = I √(2.0L/g)* is the time we assume that the cylinder is emptied so *Mg = 0*. The moment of inertia is given by the following expression:

$$I(t)=\begin{cases} \frac{1.0}{3.0}\left(M_c+M_g\right)L^2-\frac{1.0}{3.0L}\left(M_g\left(\frac{1.0}{20}gt^2\right)^3\right) & si\ \ t\le\sqrt{\frac{20L}{g}} \\ \frac{1.0}{3.0}M_cL^2 & si\ \ t>\sqrt{\frac{20L}{g}} \end{cases}. \quad (12)$$

Where *Mc* is the mass of the cylinder which will assume once ranging has been reached at time *t = I√(2.0L/g)*. On the other hand have the expression for the mass-center distance to the axis of rotation.

$$d(t)=\begin{cases} \frac{L}{20}-\left(\frac{1.0}{20}gt^2\right)\frac{M_g(t)}{M_c+M_g(t)} & si\ \ t\le\sqrt{\frac{20L}{g}} \\ \frac{L}{20} & si\ \ t>\sqrt{\frac{20L}{g}} \end{cases}. \quad (13)$$

These three terms are shown in Figs. 8, 9, 10, for three different values of granular mass *Mg = 1.0, 2.0* and *5.0g*. The angular frequency is expressed as follows:

$$\omega(t)=\frac{\left(M_c+M_g(t)\right)g\,d(t)}{I(t)}. \quad (14)$$

So the period of the pendulum is $T = 2\pi/\omega$. Shown in Fig. 11.

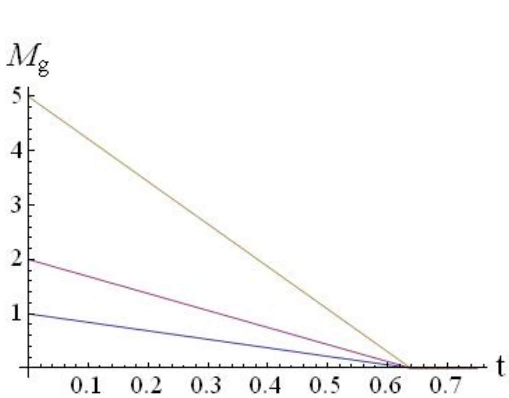

FIGURE 8. Granular mass as a function of time, expression number (11).

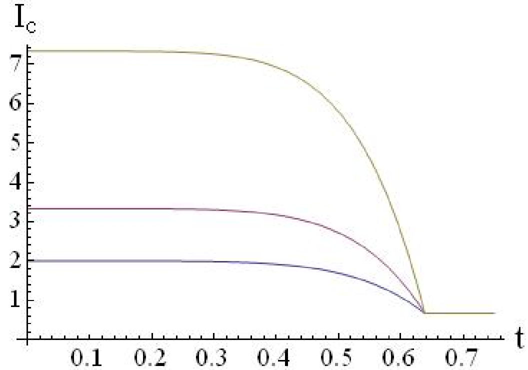

FIGURE 9. Moment of inertia as a function of time, expression expression (10).

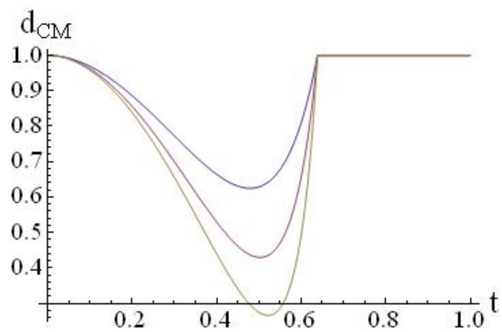

FIGURE 10. Distance from the mass center to the rotation axis as function of time, expression (11).

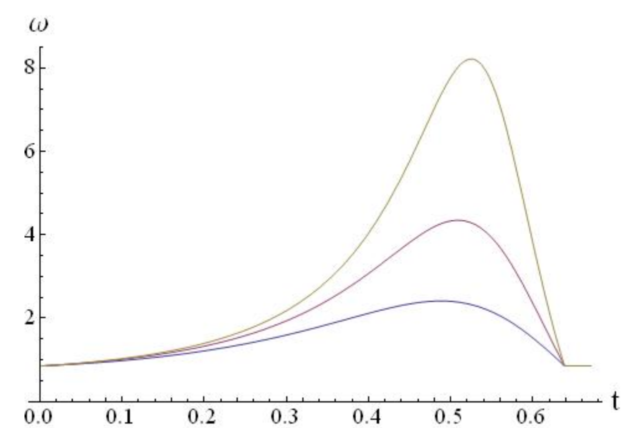

FIGURE 11. Period as function of time for the case of variable mass.

With the expressions (11-14) we done the simulation for the two cases VI) the integration interval for the first case was $0 \le t \le 1.3$, were generated $N = 500$ steps, the size of temporal displacement was $\Delta h = 0.0026$. Were evaluated the n = 100 randomly initial conditions for a range between $-35^o \le \varphi \le -35^o$ and $-1.5A \le \xi \le 1.5A$, and for the case VII) the integration interval to the second case was $0 \le t \le 2.6$, were generated N = 700 steps, the size of the temporary displacement was Δh = 0.0037. Were evaluated the n = 100 randomly initial conditions for a range between the -15°-≤ φ ≤ 15°, and *-1.5A ≤ ξ ≤ 1.5A*, where *A* is the amplitude of the oscillation.

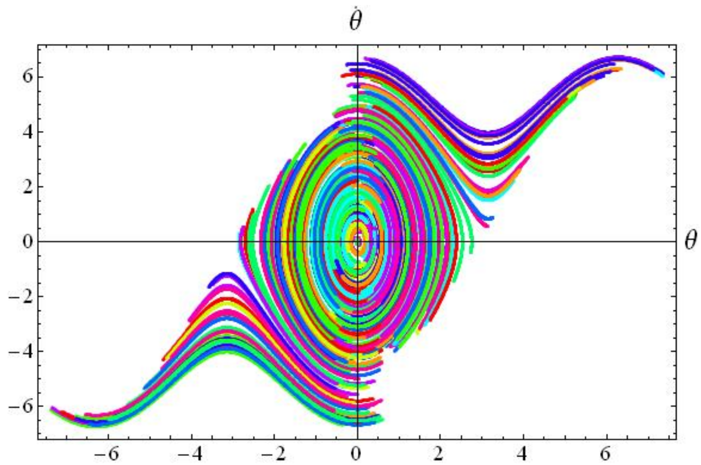

FIGURE 12. Phase diagram to damped pendulum with variable mass.

The Fig. 12 shows the phase space generated for the case VI), clearly shows the critical region and the chaotic to this more complex system, however, appear very similar phase diagrams. Fig. 13 shows the phase plane variable mass damped pendulum, given the conditions we see that this diagram shows only the region of stable equilibrium of the system. However, Fig. 14 shows the case again the case of a critical oscillation, in this case $b = b(t) = 2.0\ \omega(t)$ shows a very rapid damping, and in this case the buffer also variable as other time dependent variables.

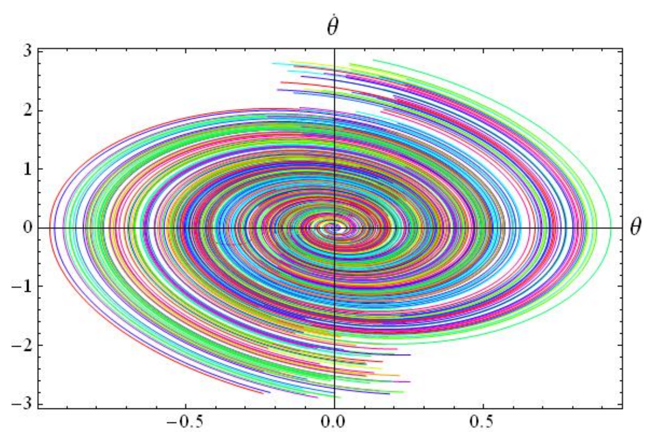

FIGURE 13. Phase diagram of the damping pendulum with mass variable, only stable region.

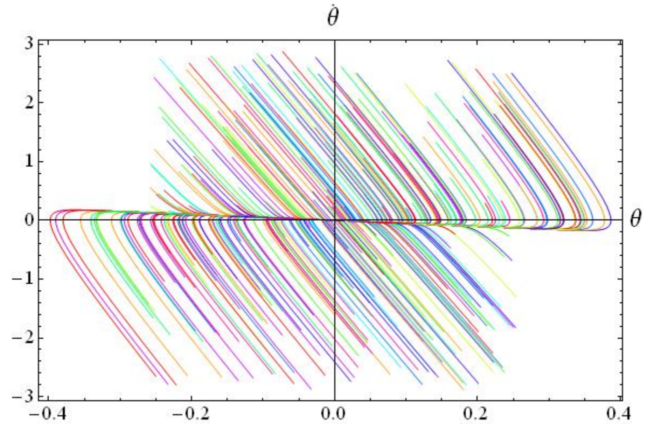

FIGURE 14. Critical damping in the case VII damping pendulum with mass variable.

V. CONCLUSIONS

There has been a very cursory study of pendulums on different systems, starting from simple approaches to complicate the problem to obtain the solution of the damping physical pendulum with variable mass, academic problem that not has been treated rigorously, and for which there aren't literature that present results to compare with our results. The results of these simulations allow us to have a computational point of view to be used to compare experimental results. It is also possible to develop a more comprehensive analysis on the chaotic regions, stable and unstable regions, branching points and different conditions for various pendulum systems presented in this work. Comparisons with experimental results are necessary but the evidence that is presented is sufficiently consistent to implement them, It is also possible propose another kind of dependence of mass flux with respect to time and oscillation to understand best the movement of pendulum.

ACKNOWLEDGEMENTS

One of the authors REH is grateful to the Universidad Autónoma Metropolitan Azcapotzalco and the Universidad Autónoma del Estado de México in the Unidad Académica Profesional de Cuautitlán Izcalli both displayed for the facilities to do this work.

REFERENCES

[1] Burden, R. L., Faires, J. D., *Numerical Analysis*, 6a ed. (Brooks/Cole Publishing Company, USA, 1997).
[2] Boyce, DiPrima, *Elementary Differential Equations and Boundary Value Problems*, 9th Ed. (Wiley, San Francisco, 2010).
[3] Braun, M., *Differential Equations and their applications*, 4th Ed. (Springer, New York, USA, 1993).

[4] Baker, L. G., Blackburn, A. J., *The Pendulum: A Case Study in Physics*, (Oxford University Press: Oxford, 2005).

[5] Nelson, A. R., Olsson, M. G., *The pendulum-Rich physics from a simple system*, Am. J. Phys. **54**, 112-121 (1986).

[6] Souza de Paula, A., Amorim, S. M., Heitor, I. F., Pereira-Pinto, *Chaos and transient chaos in an experimental nonlinear pendulum*, Journal of Sound and Vibration **294**, 585–595 (2006).

[7] Lima, F. M. S., Arun, P., *An accurate formula for the period of a simple pendulum oscillating beyond the small angle regime*, Am. J. Phys. **74**, 892-895 (2006).

[8] Camilo A. Jiménez R., Diego F. Jaramillo C., Miller J. Vargas B., *Péndulo Esférico, Forzado y Amortiguado con Masa Variable*, Revista Colombiana de Física **38**, 962-966 (2006).

[9] Chaos, U. F. and Chaos, C. L., *Comportamiento Asintótico, para el periodo del péndulo simple*, Revista Mexicana de Física **48**, 586-588 (2002).

[10] Gómez, G., Díaz, J. y Fajardo, F., *Péndulo Físico Sujeto por Resortes*, Revista Colombiana de Física **36**, 56-59 (2004).

[11] Fernández, G. M., *Péndulo de longitud variable: Experimentos*, E **53**, 120–126 (2007).

[12] Kettler, J. E., *A variable mass physical pendulum*, Am. J. Phys. **63**, 1049-1051 (1995).

[13] Szyszkowski, W., Stilling, D. S. D., *On damping properties of a frictionless physical pendulum with a moving mass,* International Journal of Non-Linear Mechanics **40**, 669–681 (2005).

[14] del Valle, G., Hernández, G., Araujo, V., Peralta, L. y Maca, S., *Péndulo físico de Masa Variable Amortiguado*, Avance de las Mujeres en las Ciencias, las humanidades y todas las Disciplinas, (UAM, México, 2011), pp. 159–168.